

STRATOSPHERIC TEMPERATURE PATTERNS DERIVED FROM NIMBUS II MEASUREMENTS

Guenter Warnecke\* and Andrew W. McCulloch

N 68-33864 Goddard Space Flight Center

Greenbelt, Maryland

19  
pages  
DX-60427  
Code

ABSTRACT

The Nimbus II medium resolution infrared radiometer (MRIR) experiment provided data for the period of May 15 to July 29, 1966. The measurements within the 15 micron carbon dioxide absorption band were processed by a large computer and printed in map form as polar stereographic and Mercator projections. The influence on the measurements by middle and upper tropospheric cloud systems was eliminated by automatic application of a specific correction model using the simultaneous measurements of the 10 - 11 micron window channel for the needed cloud top height information.

The series of horizontal stratospheric temperature patterns that can be derived from these measurements covers the northern hemisphere in late spring and early summer as well as the southern hemisphere in late fall and early winter seasons. The northern hemispheric stratosphere exhibits its very stable summerly temperature regime, while in the southern hemisphere, the stratospheric circulation is characterized by a continuous intensification of the cold polar vortex. The most striking phenomenon is an obvious asymmetry of the southern hemispheric temperature distribution with a warm cell moving cyclonically around the pole over the higher midlatitudes during the first part of the period of measurement. This apparently causes a remarkable asymmetry in the cooling pattern observed over the two months period, the

---

\* On leave from the Free University of Berlin, Germany as a National Academy of Sciences - National Research Council Senior Postdoctoral Resident Research Associate with the National Aeronautics and Space Administration.

CFSTI

H.C.  
M.F.

CAN. 13

maximum cooling of  $15^{\circ}\text{K}$  being located at  $55 - 60^{\circ}$  rather than over central Antarctica.

**STRATOSPHERIC TEMPERATURE PATTERNS DERIVED FROM NIMBUS II MEASUREMENTS**

**Guenter Warnecke and Andrew W. McCulloch**

**Goddard Space Flight Center**

**Greenbelt, Maryland**

**August 1967**

**Paper presented at the COSPAR TENTH PLENARY MEETING, July 24-29, 1967**

**London, England**

CONTENTS

	<u>PAGE</u>
ABSTRACT	111
1. INTRODUCTION . . . . .	1
2. THE ELIMINATION OF CLOUD INFLUENCE . . . . .	2
3. THE STRATOSPHERIC TEMPERATURE PATTERNS . . . . .	3
4. FINAL REMARKS . . . . .	4
5. REFERENCES . . . . .	5

# STRATOSPHERIC TEMPERATURE PATTERNS DERIVED FROM NIMBUS II MEASUREMENTS

## INTRODUCTION

One of the five Nimbus II medium resolution infrared radiometer (MRIR) detectors was sensitive over a spectral interval approximately two microns wide, centered within the 15 micron carbon dioxide absorption band (14 - 16 micron =  $720-630\text{cm}^{-1}$ ), (Ref. 1).

As a result, the maximum contributions to the outgoing radiance came from atmospheric layers at heights between 15 and 20 kilometer (2). Thus the integrated radiation temperatures were influenced not only by the lower stratospheric but, in low latitudes, by the upper tropospheric carbon dioxide as well. In the presence of dense high clouds, the tropospheric emission is replaced by the lesser emission of the colder cloud resulting in lower radiance or lower equivalent black body temperature. Therefore, the pattern of cloud systems is superimposed upon the stratospheric temperature pattern (Fig. 1) and has to be eliminated when deriving the stratospheric temperature distribution from these measurements.

The possibility of deriving stratospheric temperature patterns from 15 micron measurements was successfully shown with the TIROS VII experiment (3). In that experiment,

^ because of a smaller spectral range, the cloud attenuation was considerably smaller (although still detectable in the tropics), and a high correlation of the derived temperature patterns with those derived from conventional radiosonde measurements was established (4). However, the orbital configuration of TIROS VII did not provide measurements over the polar regions. Also, because of a poor signal-to-noise ratio averages over at least several days had to be computed to derive maps (5). The Nimbus II quasi-polar orbit and the wider spectral range of the MRIR 15 micron channel

eliminated these disadvantages and resulted in a continuous series of daily global stratospheric temperature patterns. The first results from these maps will be briefly reported here.

#### THE ELIMINATION OF CLOUD INFLUENCE

The outgoing radiances for the spectral regions and the spectral response of the Nimbus II, 10 - 11 micron and 15 micron channels were computed from the radiative transfer equation for 7 model atmospheres, for 4 different nadir angles, and for clear sky conditions and cloud tops at 9 different altitudes (6). From these calculations, corrections were determined which eliminated the attenuation of the "window" measurements by ozone and water vapor. The corrections were used to derive cloud top temperatures from these measurements assuming black body radiation. The derived cloud top temperatures were interpreted as cloud top heights by means of the proper standard atmosphere (COESA). The corrections of the 15 micron channel measurements were applied to each single scan spot.

## THE STRATOSPHERIC TEMPERATURE PATTERNS

Due to the late spring and early summer season the northern hemisphere does not exhibit marked temperature changes during the period of May 15 through July 24. The temperature distribution during this period is consistently characterized by the warm center over the North Pole and a slight meridional temperature gradient. The temperature pattern is almost symmetrical around the pole, the warmest temperature on May 21, 1966 was  $237^{\circ}\text{K}$ ,  $238^{\circ}\text{K}$  was observed on July 24, the maximum temperature of  $240^{\circ}\text{K}$  occurred around July 1, 1966 (Fig. 2).

The Mercator maps reproduced in Figures 3 and 4 demonstrate remarkably stable temperature conditions over the tropical regions throughout the ten-week period and the slight warming over the higher northern mid-latitudes. The southern hemisphere, however, is characterized by pronounced zonal temperature gradients at the beginning of the period. These decrease with time while the meridional gradients increase due to the continuous cooling over the higher southern latitudes. Details of these processes can be studied by means of the southern hemispheric maps (Fig. 5-9).

On May 21, 1966 the southern polar vortex is already well established and located over the South Pole where it remains throughout the period of observation. Its temperature structure is, however, asymmetric in the beginning. Stronger temperature gradients toward and pronounced warm centers over the South Atlantic and southern Indian Ocean characterize the temperature distribution in Figure 5. 20 days later (Fig. 6) the temperature asymmetry is almost reversed, the warmer mid-latitudes and the strong temperature gradients now being shifted toward the Australian and western Pacific side of the hemisphere. Meanwhile, the cold air center cooled by

5°K. Another 20 days later (Fig.7) the temperature over the South Pole dropped by 4 more degrees and the hemispheric temperature distribution became symmetric around the Pole. This situation was maintained until July 24 (Fig. 8). The cooling of the Antarctic stratosphere slowed down remarkably during July.

The net temperature change throughout the entire two-month period (Fig. 9) shows maxima of more than 15°K cooling south of Africa and the Indian Ocean, while the cooling over the Antarctic continent is considerably smaller. This displacement of the center of cooling toward sub-polar latitudes seems to indicate a high contribution of dynamic processes to the observed cooling pattern rather than radiative heat loss being the only governing factor in the southern hemispheric winter stratosphere.

#### FINAL REMARKS

These examples again present evidence of the feasibility of remote sensing and global mapping of stratospheric temperatures from satellite altitudes, and they also prove the usefulness of the applied model to correct for the observed cloud effect by multi-channel measurements. An atlas of all daily maps for the entire Nimbus II lifetime is under preparation.

REFERENCES:

- (1) NIMBUS II USERS' GUIDE, Nimbus Project, Goddard Space Flight Center  
Greenbelt, Maryland, July 1966
- (2) V.G.Kunde "Theoretical computations of the outgoing infrared radiance from  
a planetary atmosphere" Publication G-788, Goddard Space Flight  
Center, Greenbelt, Maryland (1967)
- (3) W.Nordberg et al. "Stratospheric Temperature Patterns based on Radiometric  
Measurements from the TIROS 7 Satellite" Space Research V, pp.782  
North-Holland Publishing Company, Amsterdam (1965)
- (4) G.Warnecke "TIROS VII 15 micron radiometric measurements and mid-stratospheric  
temperatures" in: Satellite Data in Meteorological Research,  
NCAR-TN-11, National Center for Atmospheric Research, Boulder,  
Colorado (1966)
- (5) J.S.Kennedy "An Atlas of Stratospheric Mean Isotherms Derived from TIROS VII  
Observations" Publication X-622-66-307 (1966), Goddard Space Flight  
Center, Greenbelt, Maryland
- (6) G.Warnecke "A Model for the Elimination of Cloud Contamination in Stratospheric  
Temperatures Derived from Satellite Measurements Near 15 Microns"  
Paper presented at the 1967 Spring Meeting of the American Geophysical  
Union, Washington, D.C. (to be published)

## FIGURE CAPTIONS

**Fig.1** A typical example of the photographic imagery of Nimbus II medium resolution radiometer infrared radiometer measurements in the CO<sub>2</sub> absorption band and temperatures in the atmospheric window region. High brightness of the recorded radiative flux are represented by dark grey tones, low brightness temperatures by light grey or white. The 15 micron film strip demonstrates the superposition of the cloud pattern (white, compare with the window channel picture) upon the stratospheric temperature pattern that varies from high temperatures (dark grey shades) over the Arctic to low values around 60°S.

**Fig.2** Stratospheric temperature distribution from Nimbus II measurements on July 1, 1966

**Fig.3** Stratospheric temperature distribution from Nimbus II measurements on May 21, 1966

**Fig.4** Stratospheric temperature distribution from Nimbus II measurements on July 24, 1966

**Fig.5** Stratospheric temperature distribution from Nimbus II measurements on May 21, 1966

**Fig.6** Stratospheric temperature distribution from Nimbus II measurements on June 10, 1966

**Fig.7** Stratospheric temperature distribution from Nimbus II measurements on July 1, 1966

**Fig.8** Stratospheric temperature distribution from Nimbus II measurements on July 24, 1966

**Fig. 9** Stratospheric temperature change derived from Nimbus II measurements from May 21 through July 24, 1966 in °K

NIMBUS II, MRIR  
JUNE 10, 1966

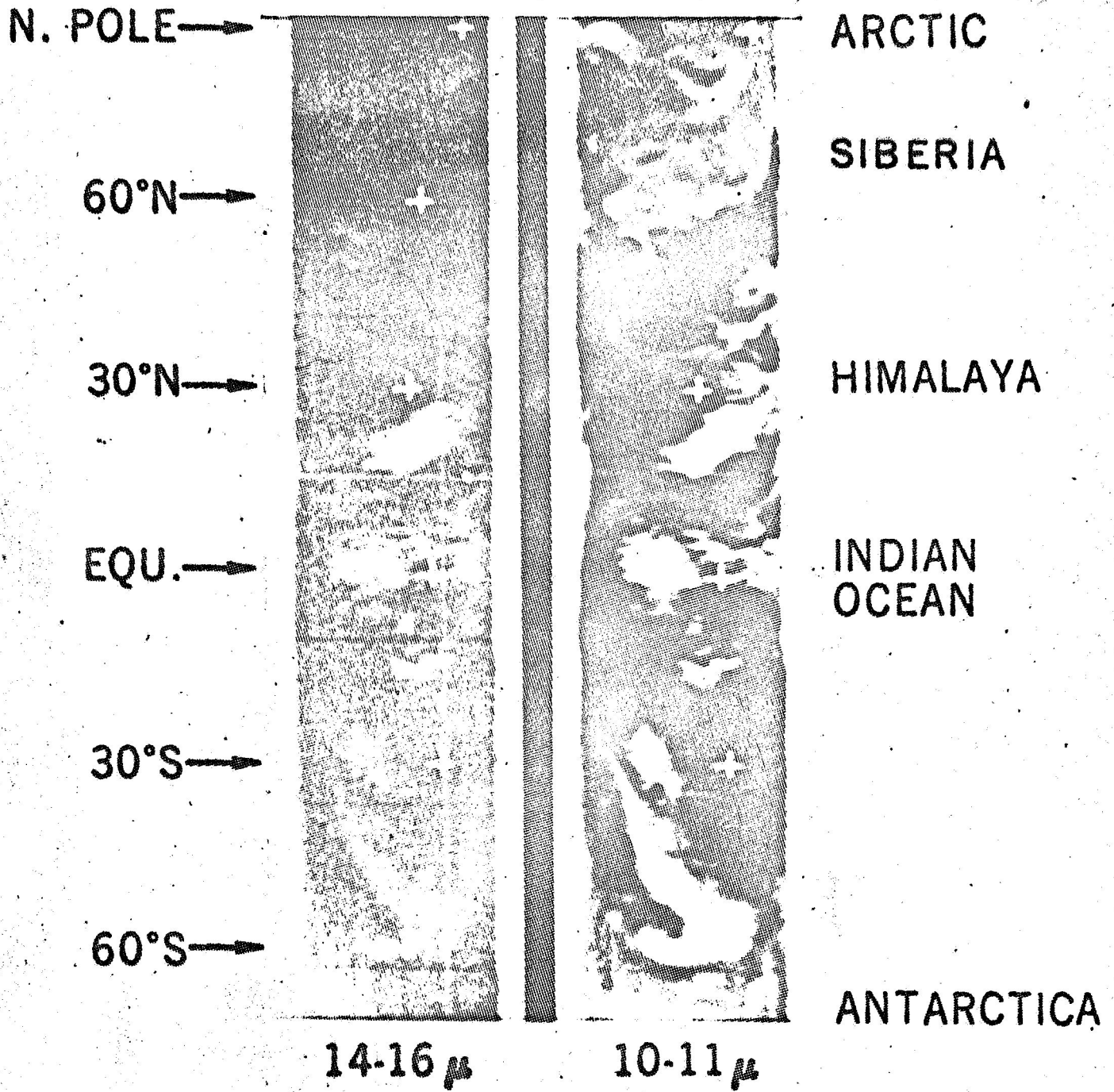
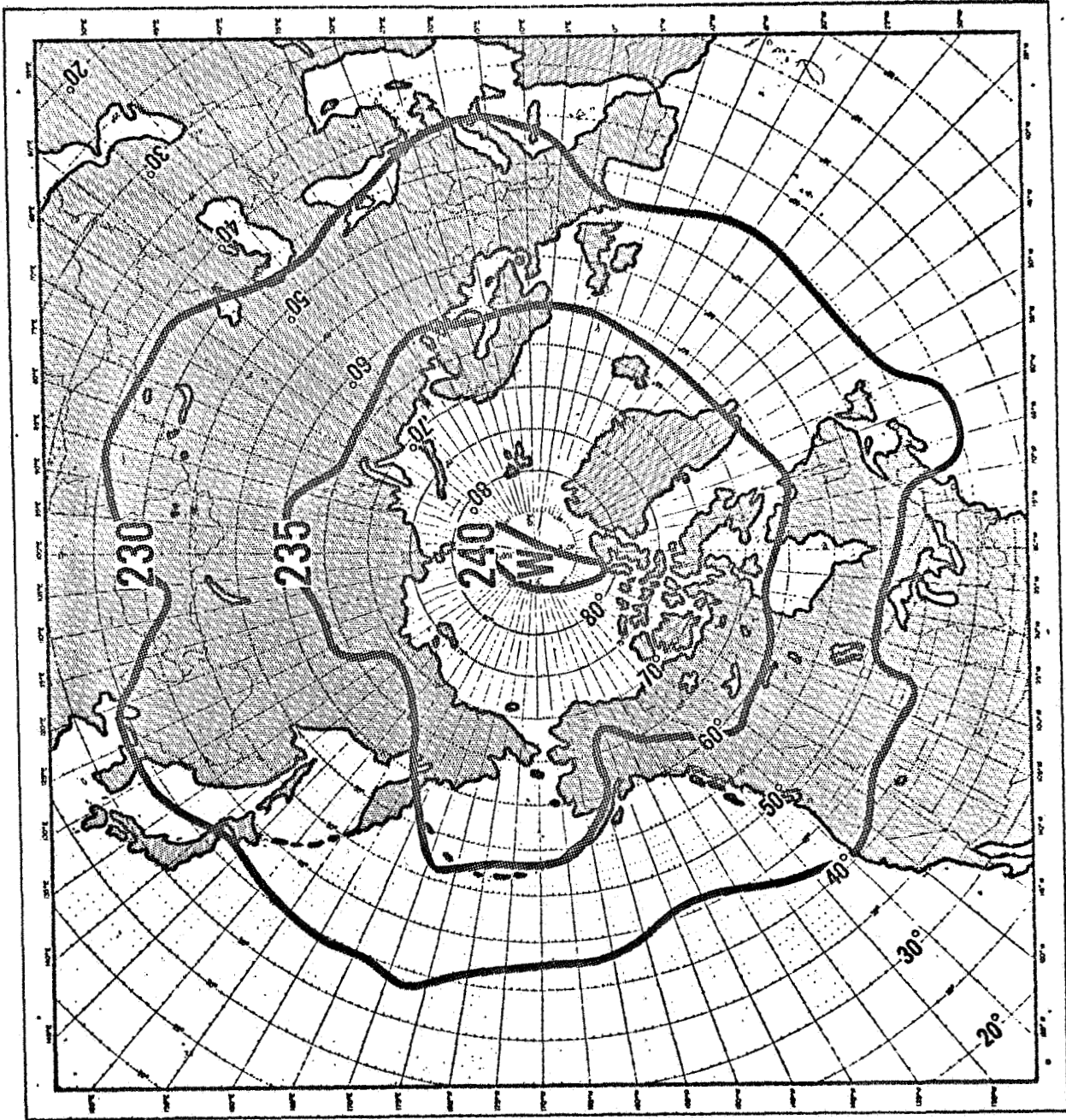


FIG. 1

STRATOSPHERIC  
TEMPERATURE  
DISTRIBUTION  
FROM NIMBUS II

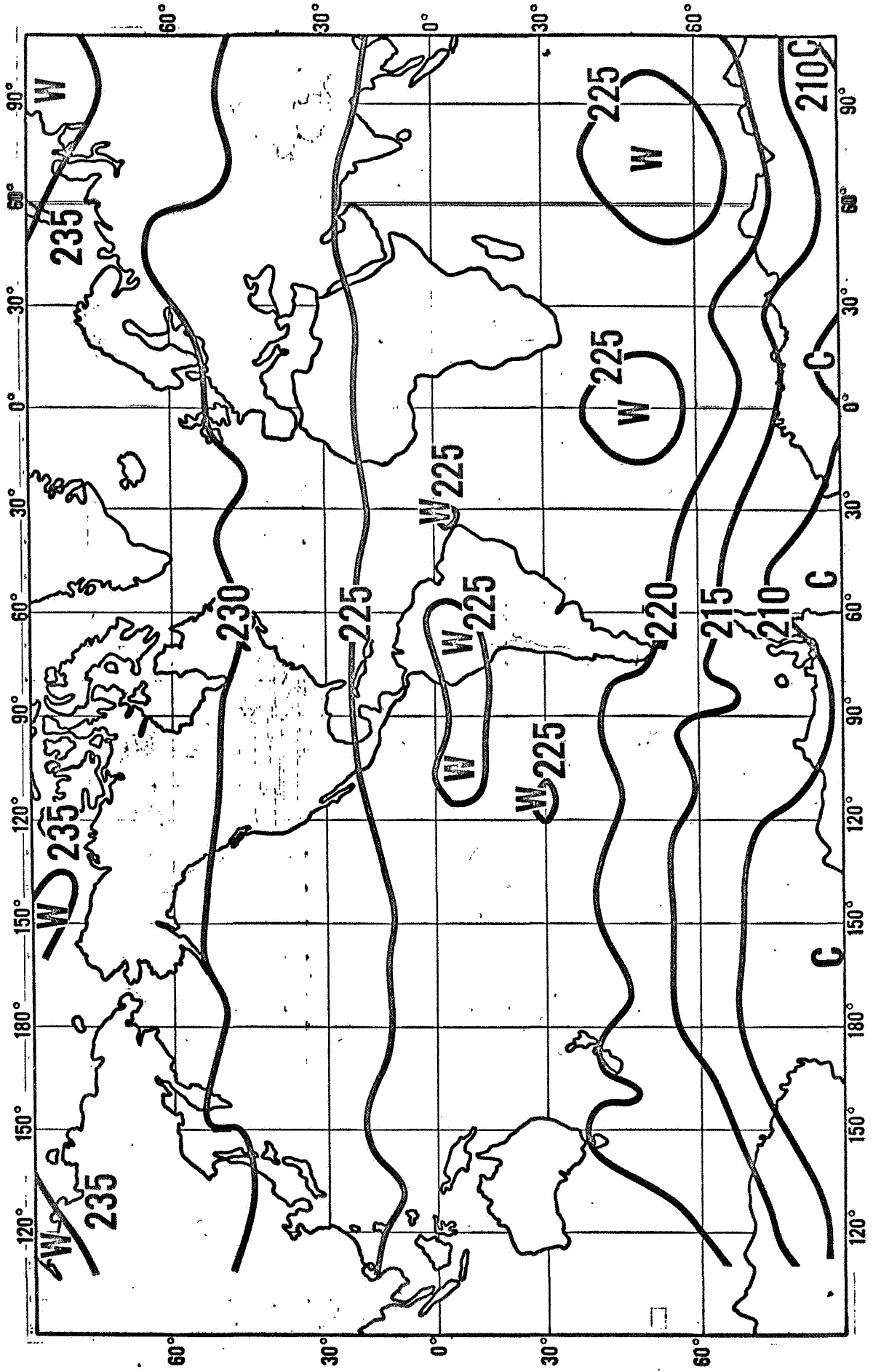
JULY 1, 1966

Fig. 2



# STRATOSPHERIC TEMPERATURE DISTRIBUTION FROM NIMBUS II

MAY 21, 1966

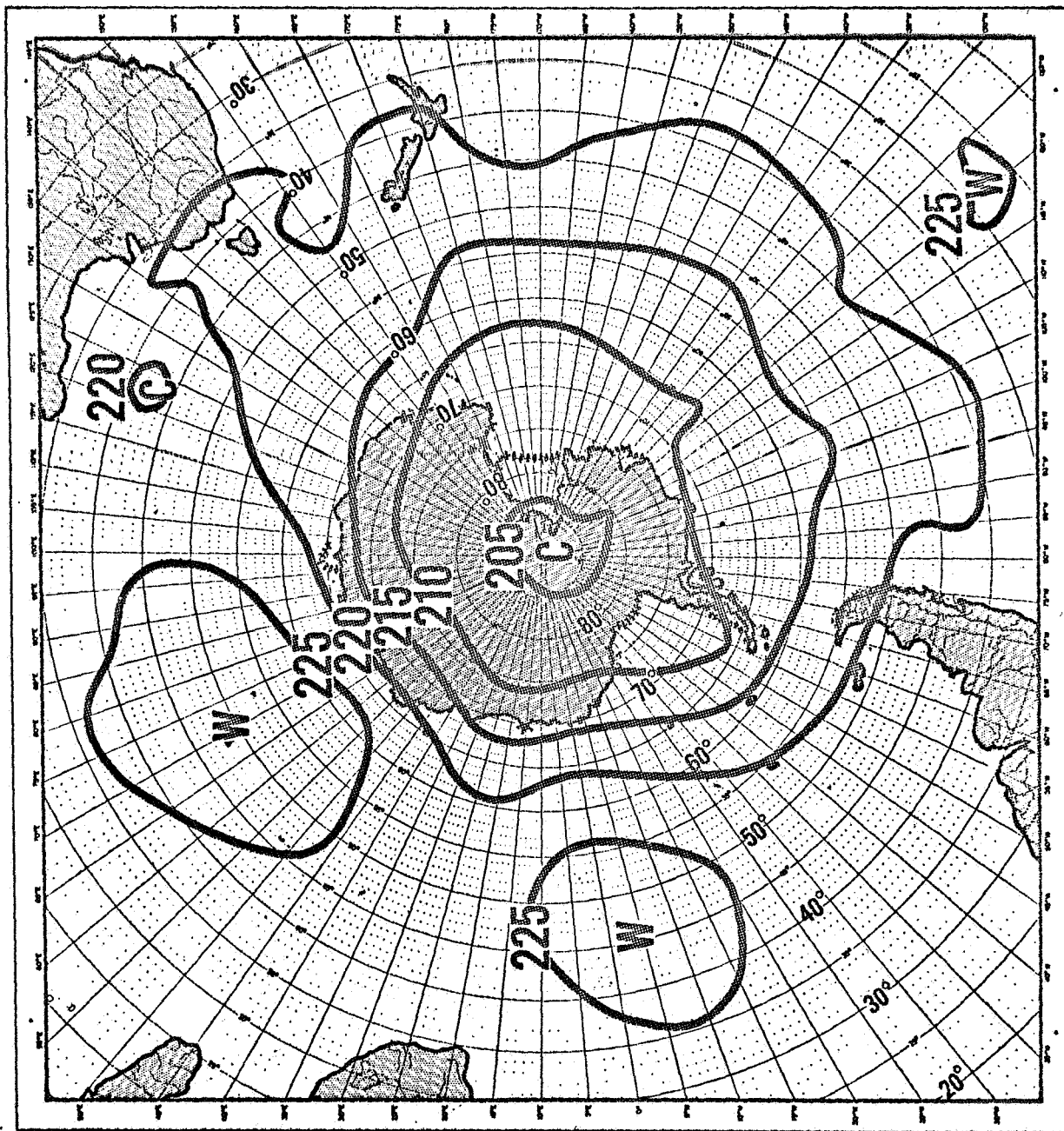




STRATOSPHERIC  
TEMPERATURE  
DISTRIBUTION  
FROM NIMBUS II

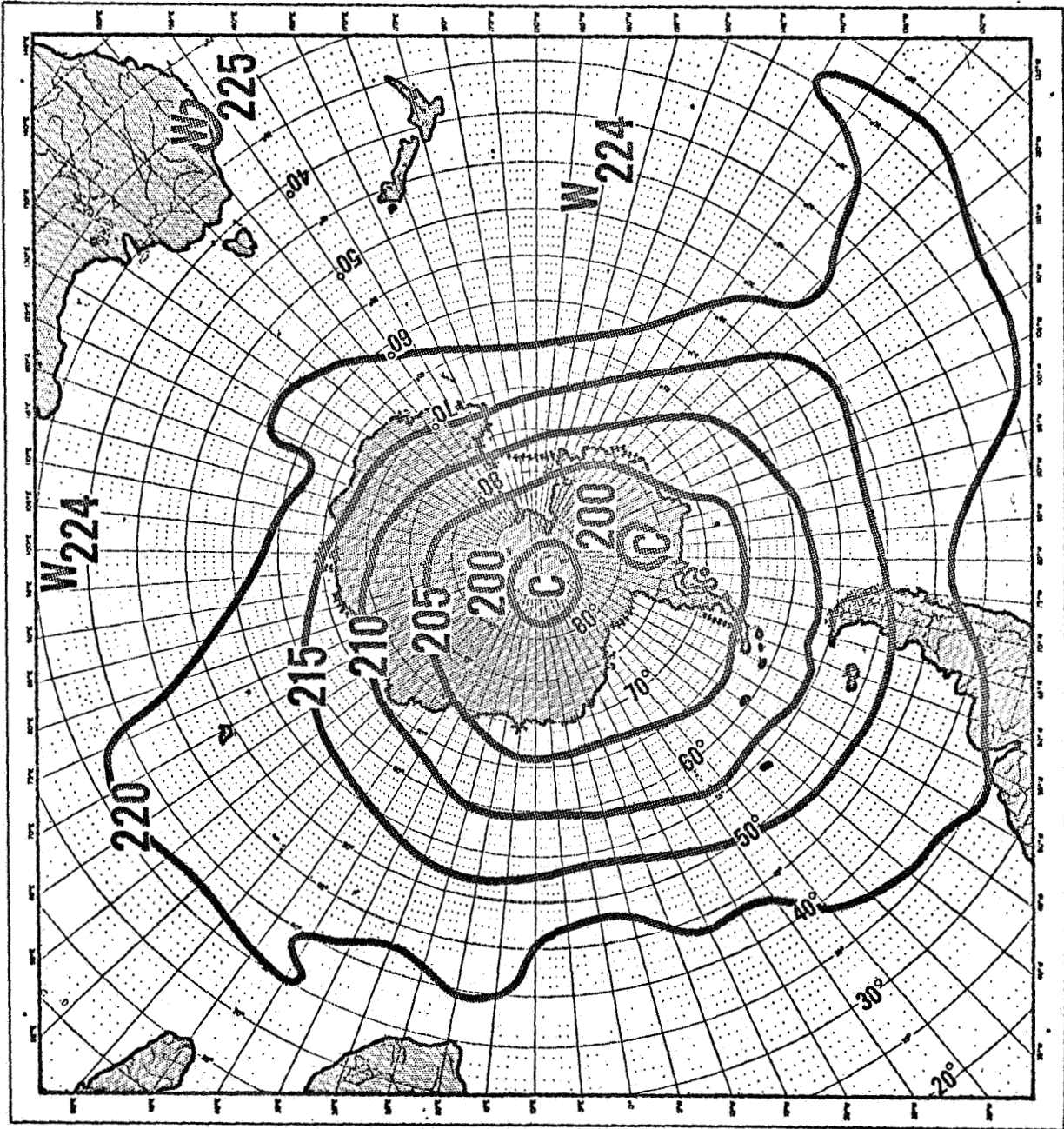
MAY 21, 1966

Fig. 5



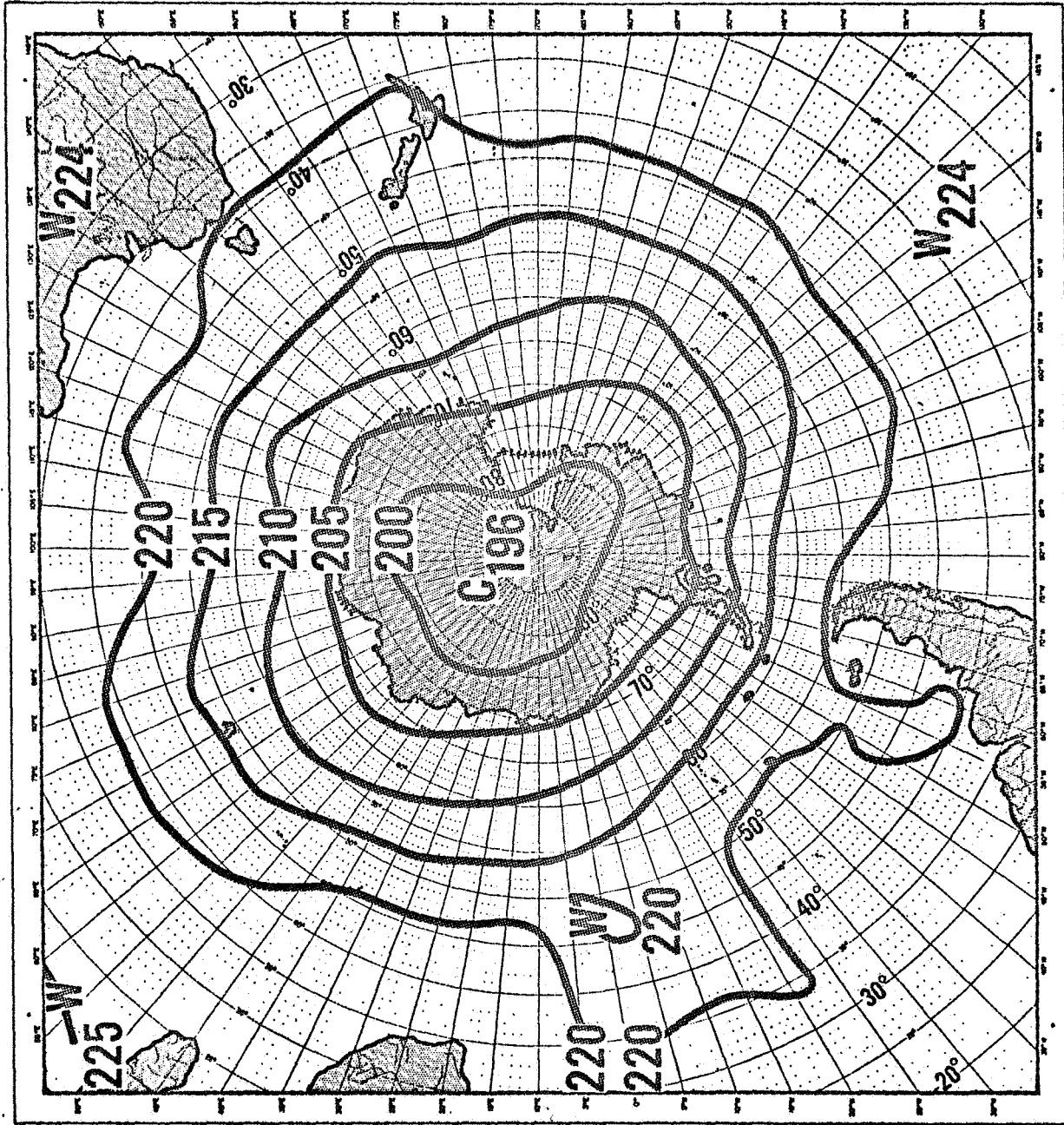
STRATOSPHERIC  
TEMPERATURE  
DISTRIBUTION  
FROM NIMBUS II

JUNE 10, 1966



STRATOSPHERIC  
TEMPERATURE  
DISTRIBUTION  
FROM NIMBUS II

JULY 1, 1966



STRATOSPHERIC  
TEMPERATURE  
DISTRIBUTION  
FROM NIMBUS II

JULY 24, 1966

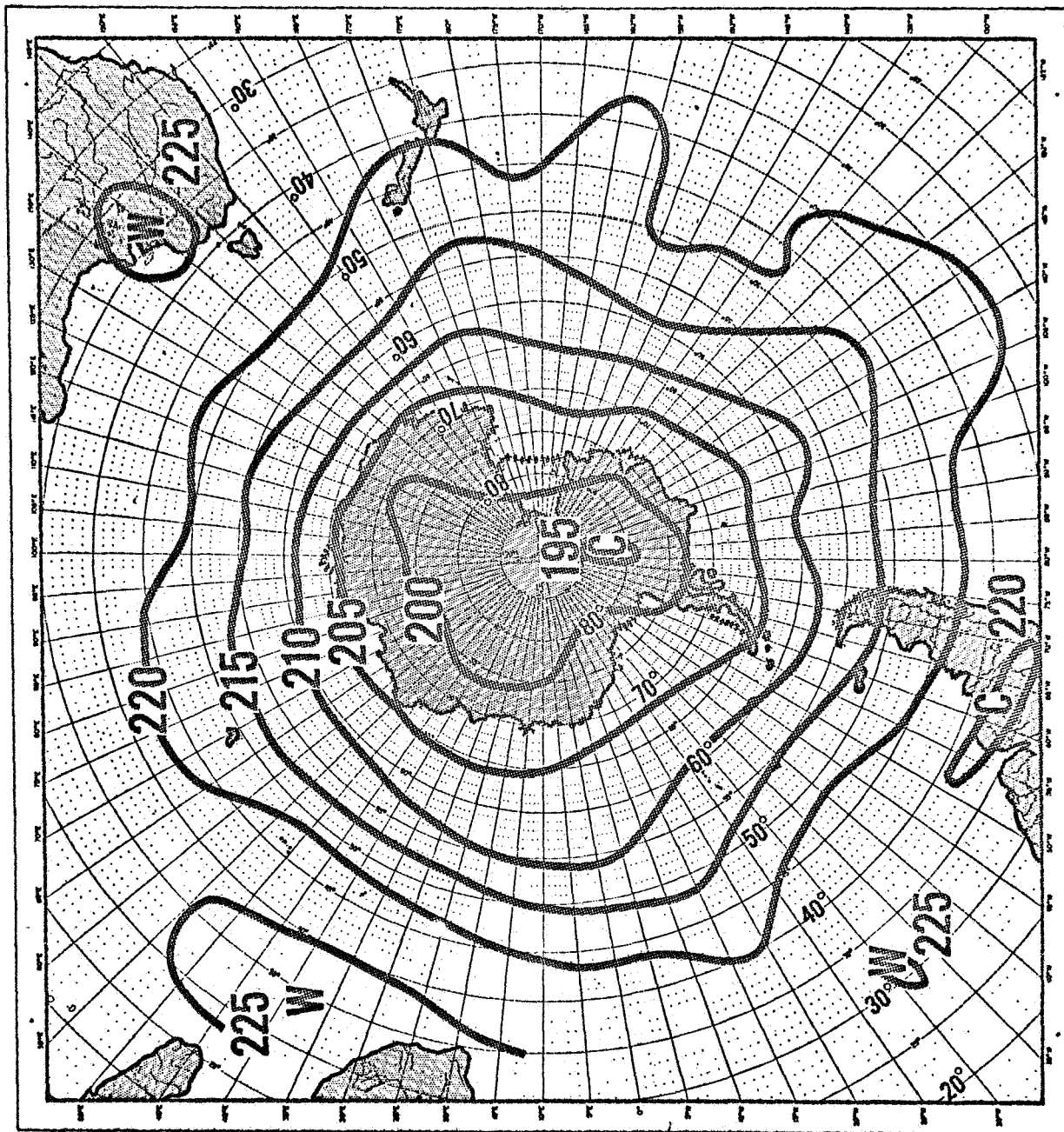


Fig. 8